The shower curtain effect in time-revesal wireless communications

Kyritsi, Persefoni; Papanicolaou, George

Publication date:
2006

Document Version
Publisher's PDF, also known as Version of record

THE SHOWER CURTAIN EFFECT IN TIME-REVERSAL WIRELESS COMMUNICATIONS

Persefoni Kyritsi[1] **and George Papanicolaou**[2]

[1]*Department of Communication Technology, Aalborg University, Denmark*
[2]*Department of Mathematics, Stanford University, USA*

ABSTRACT

Time reversal is a scheme that has its origins in wideband transmission in underwater acoustics and ultrasound, and has remarkable temporal and spatial focusing properties at the intended receiver. In this paper we are applying it to radio waves and investigate the efficiency of time reversal in a specific simulated propagation environment where the transmitter and the receiver are separated by a slab of scatterers. This type of environment relates to the shower curtain effect, and we investigate the dependence on the distance of the communicating ends from the scatterers. We find that the dominant factor is the equivalent aperture of the antenna array as determined by the size of the scatterer group.

Key words: Time reversal, spatial focusing, temporal focusing, shower curtain.

1. INTRODUCTION

Time reversal (TR) is a scheme that has its origin in wideband transmission in underwater acoustics and ultrasound [1], [2]: in TR, the signal to be transmitted is filtered through a filter that is the time reversed and phase conjugated channel impulse response (CIR). TR filtering is commonly applied in Multiple Input- Single Output (MISO) situations, i.e. where there are N_{TX} transmit antennas and one receive antenna. The resulting signal focuses tightly on the intended receiver in both space and time. Due to these properties, TR has recently appeared as a promising technique for secure, wideband, wireless communications, and the feasibility of its implementation has recently been demonstrated for radio waves [3].

In [4], [5], the efficiency of TR as a means of temporal compression was investigated by looking at the achievable reduction of the delay spread of the channel, based on actual channel measurements. The analysis showed that the efficiency of TR in reducing the perceived delay spread of the channel depends on the scattering situation around the acting transmitters and receivers. Specifically two situations were defined: the cluttered to clear scenario corresponds to the case when the intended receiver is in a less scattering environment than the acting transmitter array, whereas the clear to cluttered situation happens when the intended receiver is in the clutter.

This gave rise to an investigation of what is commonly referred to as the shower-curtain effect. The term describes the following situation: Imagine you are looking through a transparent shower curtain while taking a shower. The view from the inside out (from behind the shower curtain) is very much blurred. The view from the outside in (from some meters away from the shower curtain) is comparatively clear.

[7] has mathematically analyzed this effect in the regime of turbulent propagation. [8] has investigated the influence of the shower curtain effect on the spatial focusing properties of TR. Both papers treat the propagation environment as a random channel with known correlation properties. Specifically [8] analyzes the moments of the re-focused field around the intended receiver and shows that the time-reversed field focuses with tighter resolution around the intended receiver if the scatterers are close to the receiver, rather than when they are close to the transmitter. The parameter of interest is the size of the focal spot.

In this paper we introduce a unified framework to study the spatial and temporal focusing properties of time reversal in the presence of the shower curtain effect. Specifically we use the slab of scatterers modeling approach. We investigate the effects of bandwidth, number of transmit antennas, and transmit antenna spacing on the efficiency of TR as a means to reduce the perceived delay spread of the channel and on the achievable spatial focusing. We look not only at the size of the main focal spot, but also on the height and spacing of the focusing sidelobes.

2. TIME REVERSAL TRANSMISSION

2.1. Fundamentals of TR transmission

In the following we denote as $h(t; \underline{r}_{TX}, \underline{r}_{RX})$ the channel impulse response from a transmitter (Tx) at location $\underline{r}_{TX}$

Proc. 'EuCAP 2006', Nice, France
6–10 November 2006 (ESA SP-626, October 2006)

to a receiver (RX) at location $\underline{r}_{RX}$.

We describe the operation of a downlink TR system with N_{TX} transmit antennas as a two-stage process. The first stage is the channel estimation stage, during which each element of the transmit array obtains knowledge of the channel impulse response to the intended receiver. There are several ways in which channel estimation can be implemented (*e.g.* with a pilot signal sent by the intended receiver, or with feedback of CSI to the transmitter), which make them more or less suitable for FDD/ TDD systems. In any case, the accuracy of the CSI at the transmitter depends on the implementation details, the noise during that process, its repetition rate and the rate of change of the channel. In this paper, we are not concerned with the specifics of the channel estimation and assume that the transmitter has perfect and instantaneous CSI.

The second stage is the actual data transmission. The Tx uses the CSI it acquired during the channel estimation stage to transmit a bitstream: each of the N_{TX} elements of the transmit array transmits simultaneously the same signal $x(t)$, by filtering it through a filter $g(t)$. If the signal to be transmitted is $x(t)$, then the received signal at the Rx is $y(t)$ and can be written as

$$y(t) = \sum_{m=1}^{N_{Tx}} h(t; \underline{r}_{TX_m}, \underline{r}_{RX}) \otimes g_m(t; \underline{r}_{Txm}, \underline{r}_{RX}) \otimes x(t) \tag{1}$$

$\otimes$ denotes the convolution operator. The equivalent channel impulse response is given as

$$h_{eq}(t) = \sum_{m=1}^{N_{Tx}} h(t; \underline{r}_{TX_m}, \underline{r}_{RX}) \otimes g_m(t; \underline{r}_{TX_m}, \underline{r}_{RX}). \tag{2}$$

In pure TR, the filter $g_m(t)$ at the m-th transmit antenna is the time reversed and phase conjugated version of the channel impulse response to the intended receiver.

$$g_m^{TR}(t) = h^*(-t; \underline{r}_{TX_m}, \underline{r}_{RX}) \tag{3}$$

$(\cdot)^*$ denotes the complex conjugate of the argument $(\cdot)$. $\underline{r}_{TX_m}$ is the location of the m-th transmit antenna.

When $N_{TX} = 1$, we refer to the transmission scheme as SISO TR, whereas when $N_{TX} > 1$, we refer to the transmission scheme as MISO TR.

The equivalent channel impulse response in the case of pure TR is given as the sum of the autocorrelations of the channel impulse responses to the individual array elements. Therefore it is symmetric around $t = 0$, and it achieves its maximum at $t = 0$. This determines the synchronization between Tx and Rx, as well as the sampling time at the Rx.

The underlying assumption is that the channel transfer functions have not changed in the data transmission stage relative to the channel estimation stage.

2.2. Temporal focusing

The common measure for the temporal extent of the channel impulse response is the delay spread (DS), which is defined as the second central moment of the channel power delay profile $pdp(\tau)$:

$$DS^2 = \frac{1}{\int_{-\infty}^{+\infty} pdp(\tau) d\tau} \int_{-\infty}^{+\infty} (\tau - \bar{\tau})^2 \, pdp(\tau) d\tau \tag{4}$$

where

$$pdp(\tau) = E\left[|h(\tau)|^2\right] \tag{5}$$

$$\tau = \frac{1}{\int_{-\infty}^{+\infty} pdp(\tau) d\tau} \int_{-\infty}^{+\infty} \tau pdp(\tau) d\tau \tag{6}$$

The power delay profile is calculated as the expected value of the power of the channel impulse response within the local area of the transmitter/ receiver. Large delay spread leads to irreducible bit error rate (BER), and is therefore a fundamental limitation for wireless systems [10].

Pure TR in a SISO situation does not reduce the perceived delay spread of the channel [11]. It can do so in a MISO scenario due to the incoherent addition of the responses from the various transmit elements at delays $\tau \neq 0$. We investigate the perceived delay spread that can be achieved after the application of TR at the transmitter, by applying the above calculation to the corresponding equivalent channel impulse responses.

2.3. Spatial Focusing

Let us assume that the system performs TR with a view to communicating with an intended receiver that is located at $\underline{r}_{RX}$. We are interested in the amount of interference this operation causes at a location at distance $\underline{d}$ away from the intended receiver, *i.e.* at a location $\underline{r}' = \underline{r}_{RX} + \underline{d}$.

Low interference power at location $\underline{r}'$ would mean that it would be possible to simultaneously send data to both locations $\underline{r}$ and $\underline{r}'$, without impairing each individual communications link. Alternatively, the received power away from the target is a measure of the system's probability of intercept: low power at a distance $\underline{d}$ away from the intended receiver indicates that an eavesdropper at that location would not be able to successfully intercept the content of the communication.

The equivalent channel impulse response at location $\underline{r}'$ is given as

$$h_{eq}(t; \underline{r}') = \sum_{m=1}^{N_{Tx}} h(t; \underline{r}_{TX_m}, \underline{r}') \otimes g_m(t) \tag{7}$$

where $h(t; \underline{r}_{TX_m}, \underline{r}')$ indicates the channel impulse response from the m-th transmitter to $\underline{r}'$.

Assuming a perfectly synchronous system, and keeping in mind that the the equivalent channel impulse response on the intended receiver in pure TR achieves its maximum at $\tau = 0$, we concentrate on the value of the interference at that sampling instant:

$$IF_{t=0}(\underline{r}') = |h_{eq}(0; \underline{r}')|^2 \tag{8}$$

Alternatively we can look at the maximum level of received power at any location and define

$$IF_{MAX}(\underline{r}') = max|h_{eq}(t; \underline{r}')|^2. \tag{9}$$

3. CHANNEL MODEL

The channel model is shown in Fig. 1.

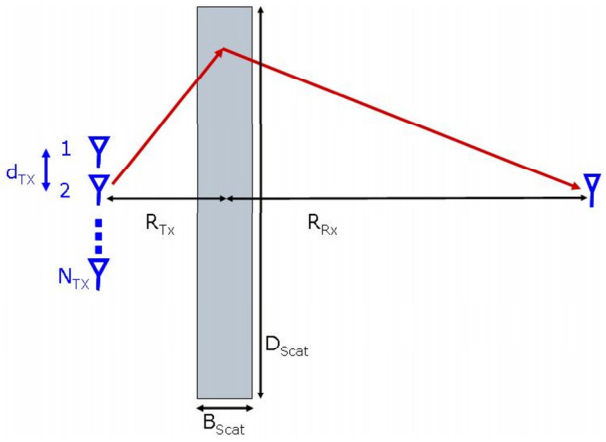

Figure 1. Channel model

We assume that we have a uniform linear array of N_{TX} along the y-axis, where adjacent elements are separated by d_{TX}. The array is placed at $x = -R_{TX}$, and centered around $y = 0$.

There are N_{scat} scatterers uniformly distributed over a rectangular area with dimensions $B_{scat} \times D_{scat}$ (along the x- and y- axes respectively). This slab is centered around $x = 0, y = 0$.

The receiver is located at the point $(R_{RX}, 0)$. In terms of spatial focusing, we investigate the performance of TR on a grid of points around the receiver, centered at the receiver location. This grid contains n_x (n_y) regularly spaced points with separation d_x (d_y) along the x-(y-) axis.

The carrier frequency of the transmission is f_c, and the bandwidth is BW. The 2-dimensional channel model used in this work is similar to the one proposed in [6], with a slight modification of the geometry. A ray-based approach is used to calculate the channel impulse response from each transmit element to any point on the grid around the receiver by summing the scattered or reflected contributions. In this paper, only single scattering is considered. The channel transfer function from any transmitter at location $\underline{r}_{tx}$ to any location $\underline{r}_{rx}$ is given by

$$h(t, \underline{r}_{tx} \rightarrow \underline{r}_{rx}) = \sum_{l=1}^{N_{scat}} \Gamma_l \frac{exp(-j\frac{2\pi}{\lambda}(d_{\underline{r}_{tx}\underline{s}_l} + d_{\underline{s}_l\underline{r}_{rx}}))}{[d_{\underline{r}_{tx}\underline{s}_l} + d_{\underline{s}_l\underline{r}_{rx}}]^{\gamma/2}} \delta(t - \tau_l), \tag{10}$$

where

- λ is the wavelength of the carrier frequency f_c. This approximation holds for small relative bandwidths.
- Γ_l is the complex scattering coefficient of the l-th scatterer. The in-phase and quadrature components of Γ_l are taken to be independent, Gaussian random variables with mean 0 and variance 1.
- $\tau_l = \frac{(d_{\underline{r}_{tx}\underline{s}_l} + d_{\underline{s}_l\underline{r}_{rx}})}{c}$ is the time of arrival of the path from the l-th scatterer.
- $d_{\underline{r}_{tx}\underline{s}_l}$ is the distance between a transmitter at location $\underline{r}_{tx}$ and a scatterer at location $\underline{s}_l$.
- $d_{\underline{s}_l\underline{r}_{rx}}$ is the distance between a scatterer at location $\underline{s}_l$ and a receiver location $\underline{r}_{rx}$.

The response is appropriately filtered to the bandwidth of interest.

For our investigations of the shower curtain effect, we keep the dimensions of the slab constant and vary R_{TX}, so that

- Clear to cluttered:$R_{TX} > R_{RX}$
- Cluttered to clear:$R_{TX} < R_{RX}$

Table 1 summarizes the parameters that are kept constant for our simulations and gives their corresponding values. The simulation was repeated for 20 realizations of the scatterer location/ scattering coefficients, and the results are averaged over these channel realizations.

4. EFFECT OF DISTANCE FROM THE SHOWER CURTAIN

We investigate the spatial and temporal focusing properties of time reversal as a function of the transmitter/ receiver distance from the slab of scatterers. We use an 8-element transmit antenna array, with an inter-element separation of 1λ. The transmitter and receiver are initially placed at equal distances from the slab of scatterers and we investigate the effect of changing this distance. We then look at the clear to cluttered and cluttered to clear scenarios. The bandwidth was taken to be 200MHz. As our measure of comparison we use the interference as defined in (8). The simulations show that we get similar results by using the definition of interference given in (9).

Table 1. Parameter Settings

Variable name	Symbol	Value
Carrier frequency	f_c	5GHz
Wavelength	λ	6cm
Bandwidth	BW	200 or 20 MHz
Slab width	B_{scat}	4000λ
Slab height	D_{scat}	40000λ
No of scatterers	N_{scat}	1000
Power roll-off factor	γ	2
No of repetitions	N_{rep}	20
No of transmit antennas	N_{TX}	8 or 4
Separation of TX antennas	d_{TX}	1λ or 2λ
Number of grid points	n_x, n_y	41
Grid cell size	d_x, d_y	0.1λ

4.1. Spatial Focusing

Fig. 2 shows how the spatial focusing changes for transmitters and receivers that are at equal distances from the slab of scatterers, as this distance increases. We observe that the spatial focusing along the x-axis deteriorates as the distance increases. However the increase in the distance reduces the height of the side-lobes along the y-axis.

Fig. 3 shows how the spatial focusing changes in the cluttered to clear scenario. We observe that the spatial focusing along the y-axis deteriorates as the distance increases, i.e. the main focal spot becomes wider. However the increase in the distance reduces the width and height of the side-lobes along the y-axis.

Fig. 4 shows how the spatial focusing changes in the clear to cluttered scenario. We observe that the spatial focusing along the y-axis deteriorates as the distance increases, i.e. the main focal spot becomes wider. Also as the distance increases, there are more and more significant sidelobes along the y-axis.

4.2. Temporal Focusing

The measure of comparison for the temporal focusing properties of time reversal is the ratio of the delay spread of the equivalent channel after MISO TR over the delay spread of the original channel impulse response. The delay spread of the original channel was in the order of 0.8-1.3μsecs. The delay spread of the original channel was reduced as the distance of either the transmitter or the the receiver from the slab of scatterers increased. The reduction in delay spread after the application of MISO-TR was in the order of 50%, which is consistent with the experimental results shown in [5]. However we have not been able to find a dependence of the temporal focusing efficiency on the scattering situation.

(a) Spatial focusing for $R_{TX} = R_{RX} = 2500\lambda$

(b) Spatial focusing for $R_{TX} = R_{RX} = 5000\lambda$

(c) Spatial focusing for $R_{TX} = R_{RX} - 10000\lambda$

Figure 2. Effect of distance from the slab on the spatial focusing properties of time reversal

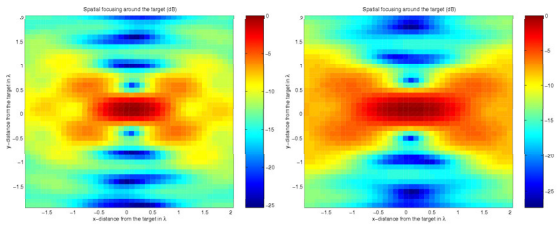

(a) Spatial focusing for $R_{TX} - 2500\lambda, R_{RX} = 5000\lambda$

(b) Spatial focusing for $R_{TX} - 2500\lambda, R_{RX} - 10000\lambda$

Figure 3. Cluttered to clear scenario

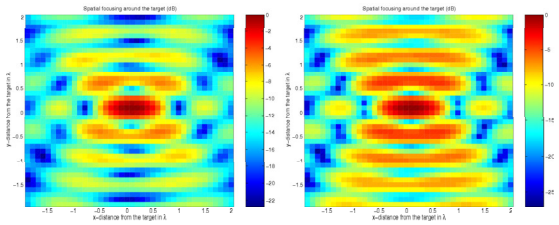

(a) Spatial focusing for $R_{TX} - 5000\lambda, R_{RX} = 2500\lambda$

(b) Spatial focsuing for $R_{TX} - 10000\lambda, R_{RX} - 2500\lambda$

Figure 4. Clear to cluttered scenario

5. EFFECT OF BANDWIDTH

We investigate the spatial focusing properties of time reversal as a function of the signal bandwidth. We use an 8-element transmit antenna array, with an inter-element separation of 1λ. The transmitter array is placed at $x = -2500\lambda$, and we observe the spatial focusing around $x = 2500\lambda$ (transmitter and receiver are equi-distant from the slab of scatterers). Fig. 5 shows the spatial focusing around the receiver for a bandwidth of 20MHz. As a measure of comparison we use the definition of (8), but using the maximum interference level would give comparable results.

The comparison of this figure with the corresponding one for a bandwidth of 200MHz clearly shows that increasing the signal bandwidth improves the spatial focusing properties of time reversal. However even with a bandwidth of 20MHz (as currently used by several WLAN systems) significant spatial focusing can be achieved.

6. EFFECT OF ARRAY SIZE

We investigate the spatial focusing properties of time reversal as a function of the array size, *i.e.* as a function of the number of transmit antennas and their separation. We specifically look at the following three transmit antenna configurations:

1. 8-element antenna array with 1λ interelement spacing.

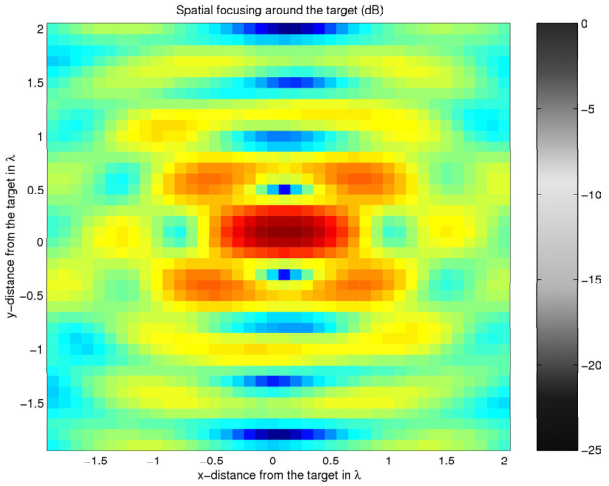

Figure 5. Spatial focusing around the target with a bandwidth of 20MHz

2. 4-element antenna array with 1λ interelement spacing.

3. 4-element antenna array with 2λ interelement spacing.

The transmitter array is placed at $x = -2500\lambda$, and we observe the spatial focusing around $x = 2500\lambda$ (transmitter and receiver are equi-distant from the slab of scatterers). Fig. 6 shows the spatial focusing around the receiver for the last two antenna configurations. As a measure of comparison we use the definition of (8), but using the maximum interference level would give comparable results.

The results are similar for all antenna configurations. The expectation would have been that larger antenna arrays (in terms of number of elements or antenna separation) would have resulted in better spatial focusing because of larger array aperture. The results indicate that the perceived aperure is dominated by the size of the slab of scatterers which is the same for all configurations and much larger than any of the individual array sizes.

With respect to the temporal focusing, the results indicate the smaller arrays are less effective in reducing the delay spread of the equivalent channel after the application of TR.

7. CONCLUSIONS AND FUTURE WORK

In this paper, we introduced a unified framework to study the spatial and temporal focusing properties of time reversal in the presence of the shower curtain effect. Specifically we used the slab of scatterers modeling approach, which is a common way to model the wireless channel.

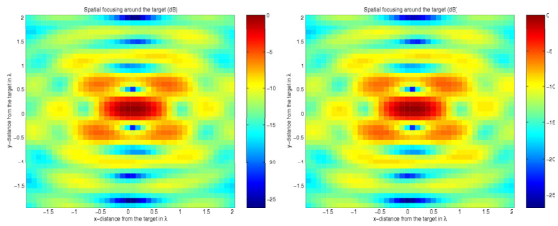

(a) $N_{TX} = 4, d_{TX} = 1\lambda$ (b) $N_{TX} = 4, d_{TX} = 2\lambda$

Figure 6. Effect of array size

We observed that the application of MISO-TR in an 8×1 system can reduce the perceived the delay spread of the channel by a factor of 2 (for propagation environments of dimensions similar to those in our experiment). However we could not see a dependence of the temporal focusing on the relative scattering situation around the transmitter and the receiver. Possibly more accurate scattering layouts (ring of scatterers, inclusion of multiple scattering) will be more efficient in investigating this effect.

We also investigated the spatial focusing properties of MISO-TR as a function of the distance of the transmitter/ receiver from the scatterers. similarly to the literature we observed that tighter spatial focusing is achieved when the scatterers are close to the intended receiver. This holds for both the directions (x- and y). We looked not only at the size of the main focal spot, but also on the height and spacing of the focusing sidelobes.

It is interesting to point out that the results discussed in this paper seem to contradict the discussion in [11], which has shown that both the temporal and the spatial focusing properties of TR improve as the number of transmitters and/ or the antenna spacing increase. However the channel model in [11] assumed separability of the channel correlation around the transmitter and the receiver, a property that is known not to hold in the slab of scatterers approach.

ACKNOWLEDGMENTS

The work of P. Kyritsi and G. Papanicolaou was supported partially by grants NSF: OMS-0354674-001 and ONR: N00014-02-1-0088.

REFERENCES

[1] M. Fink, "Time reversed acoustics," in *Physics Today*, March, pp. 33-40, 1997.

[2] M. Fink, "Time-reversed acoustics," in *Scientific American*, November, pp. 91-97, 1999.

[3] G. Lerosey, J. de Rosny, A. Tourin, A. Derode, G. Montaldo, and M. Fink, "Time Reversal of electromagnetic waves," in *Physical Review Letters*, no 92, 2004.

[4] P. Kyritsi, G. Papanicolaou, P. Eggers and A. Opera, "MISO time reversal and delay spread compression for FWA channels at 5 GHz," in *Antennas and Wireless Propagation Letters* vol. 3, pp. 96-99, 2004.

[5] P. Kyritsi, G. Papanicolaou, P. Eggers, and A. Oprea, "Time reversal techniques for wireless communications," in *Proc. IEEE 60th Vehicular Technology Conference*, Sept. 2004.

[6] C. Oestges, A. D. Kim, G. Papanicolaou, A. J. Paulraj, "Characterization of space-time focusing in time-reversed random fields," in *IEEE Trans. Antennas Propagat.*, vol. 53, no 1, part 2, pp. 283-293, Jan. 2005.

[7] A. Fannjiang, "Information Transfer in Disordered Media by Broadband Time Reversal: Stability, Resolution and Capacity," e-print: arxiv.org/abs/physics/0509158.

[8] A. Ishimaru, S. Jaruwatanadilok, and Y. Kuga, "Time reversal in random media and super resolution with shower curtain effects and backscattering enhancement," in Proc. URSI General Assembly Meeting 2005.

[9] A. Ishimaru, "Wave propagation and scattering in random media," IEEE Press, 1997.

[10] J. Chuang, "The Effects of Time Delay Spread on Portable Radio Communications Channels with Digital Modulation," in *IEEE Journal on Selected Areas in Communications*, Vol. 5, no. 5, June 1987, pp. 879 -889.

[11] P. Kyritsi, and G. Papanicolaou, "Time-Reversal: Spatio-temporal focusing and its dependence on the channel properties," submitted for publication in *IEEE Trans. on Antennas and Propagation*.